

## Electronic Supplementary Information

### A microfluidic organic transistor for reversible and real-time monitoring of H<sub>2</sub>O<sub>2</sub> at ppb/ppt levels in ultrapure water

Kohei Ohshiro <sup>a</sup>, Yui Sasaki <sup>a</sup>, Qi Zhou <sup>a</sup>, Pierre Didier <sup>a,b</sup>, Takasuke Nezaki <sup>c</sup>, Tomoharu Yasuie <sup>c</sup>, Masao Kamiko <sup>a</sup> and Tsuyoshi Minami <sup>\*a,b</sup>

---

<sup>a</sup> Institute of Industrial Science, The University of Tokyo, 4-6-1 Komaba, Meguro-ku, Tokyo, 153-8505, Japan

Corresponding author: tminami@iis.u-tokyo.ac.jp

<sup>b</sup> LIMMS/CNRS-IIS(UMI2820), The University of Tokyo, 4-6-1 Komaba, Meguro-ku, Tokyo, 153-8505, Japan

<sup>c</sup> Kurita Water Industries Ltd., 4-10-1 Nakano, Nakano-ku, Tokyo, 164-0001, Japan

#### Contents

1. General	S2
2. Fabrication and electrical measurement of the OFET-based sensor	S2
3. Characterization of the extended-gate electrode	S4
4. Electrical detection of H <sub>2</sub> O <sub>2</sub>	S4
5. DFT Calculation of dipole moment	S7
6. Investigation of the functionalized extended gate after the oxidation	S7
7. Selectivity	S8
References	

## 1. General

### Reagents and materials

Reagents and solvents utilized in this study were commercially available and used as supplied. 4-Mercaptophenylboronic acid (4-MPBA), 1,2-dichlorobenzene, and poly{2,5-bis(3-tetradecylthiophen-2-yl)thieno[3,2-*b*]thiophene} (PBTTT-C14) were obtained from Merck KGaA. Tetradecylphosphonic acid (TDPA), 4-hydroxybenzene thiol (4-HBT), 2,3-dichloro-5,6-dicyano-1,4-benzoquinone (DDQ), and benzoyl peroxide (BPO) were purchased from Tokyo Chemical Industry Co., Ltd. The target species and a conductive paste purchased from FUJIFILM Wako Pure Chemical Industries, Ltd. were *tert*-butyl hydroperoxide, sodium nitrate, sodium hypochlorite, potassium hydroxide, and a silver paste (model: D-500). Methanol was obtained from Kanto Chemical Co. Inc. The target species supplied by Kurita Water Industries Ltd. was hydrogen peroxide. Poly(dimethylsiloxane) (PDMS) (model: SILPOT 184 w/c) and negative SU-8 3050 photoresist were obtained from Dow Corning Toray Co., Ltd. and MicroChem Co., respectively. For deposition of electrodes, aluminum (Al) wire (1φ) and gold particle (Au) were obtained from Furuuchi Chemical Co., Ltd. and Tanaka Kikinzoku Kogyo Co., Ltd., respectively. For electrical measurements, an Ag/AgCl reference electrode (model: RE-1B) and a Pt wire counter electrode were obtained from BAS Inc. Glass substrates (model: Eagle XG, 2 cm × 2.5 cm) were purchased from Corning, Inc. An amorphous fluoropolymer CYTOP™ (model: CTL-809M) with perfluorotributylamine and a polyethylene naphthalate (PEN) film were supplied from AGC Co., Ltd. and TOYOBO Co., Ltd., respectively. Milli-Q water (18.2 MΩ cm) was used to prepare aqueous solutions for all experiments.

### Measurements

The extended-gate Au electrodes were characterized by using an AC-2 (Riken Keiki, Co.) for photoelectron yield spectroscopy measurement in air. In addition, X-ray photoelectron spectroscopy (XPS) (a PHI Quantera spectrometer, ULVAC-PHI, Inc.) was applied to determine the SAM modification on the extended-gate electrode. Molecular densities on the extended-gate electrode were estimated by using linear sweep voltammetry (LSV) (an SP-300 potentiostat, Biologic). All transistor characteristics were evaluated using a semiconductor parameter analyzer (Agilent, 4156B). The electrical measurement of the OFET was carried out using a probe station (Oyama Co., Ltd.) with a shield box to avoid photoexcitation of the semiconductive layer.<sup>1</sup> A two-channel vacuum pump equipped with a flow meter (Argos) was employed for the continuous measurement.

## 2. Fabrication and electrical measurement of the OFET-based sensor

### Fabrication scheme of the OFET

The organic field-effect transistor (OFET) was fabricated on an eagle glass substrate that was washed with piranha solution (H<sub>2</sub>O<sub>2</sub>:H<sub>2</sub>SO<sub>4</sub> = 1:4 (v/v)). A gate electrode (Al, 30 nm in thickness) was deposited on the eagle glass substrate by utilizing vacuum thermal deposition equipment (SVC-700TMSG/SVC-7PS80, SANYU Electron) with a shadow mask. Next, an aluminum oxide layer was formed by oxidation

of the Al electrode using a reactive ion etching (RIE) system (SAMCO RIE-10NR). The treated substrate was immersed in a 2-propanol solution containing (TDPA, 10 mM) for 15 h at 25 °C, followed by washing by 2-propanol and drying with N<sub>2</sub> gas. Subsequently, the substrate was baked at 110 °C for 30 min. After this period, vacuum thermal deposition was performed to fabricate the source and drain gold electrodes (30 nm in thickness) using a shadow mask. Moreover, 0.3 μL of a 1,2-dichlorobenzene solution containing PBTTC-C14 (0.0125 wt%) was drop-casted onto the channel region (width: 50 μm, length: 1000 μm) of the OFET, followed by a baking process at 160 °C for 10 min. Finally, the surface of the substrate was fully spin-coated by using a MIKASA SPINCOATER 1H-D7 with a fluorinated polymer solution made of CYTOP™ (CTL-809M in CT-Solv.180, ratio 1 : 1 (v/v)) and then baked at 110 °C for 10 min.

### **Basic characteristics of the OFET**

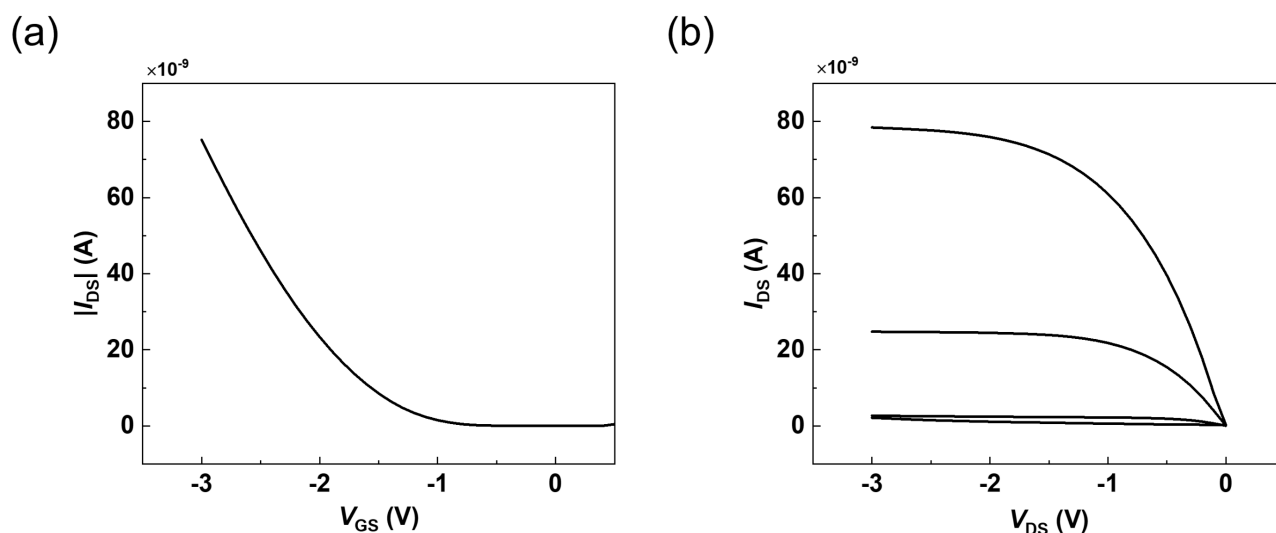


**Fig. S1** (a) Transfer and (b) output characteristics of the OFET.

### **Fabrication of the extended-gate electrode**

A sensing portion made of an Au electrode (area: 15 mm<sup>2</sup>, thickness: 100 nm) was fabricated on the PEN film (125 μm in thickness) by using vacuum thermal deposition equipment. The extended-gate electrode was washed with methanol and dried with N<sub>2</sub> gas, followed by immersion into a methanol solution containing 4-MPBA (10 mM) or 4-HBT (10 mM) for 1 h at 25 °C. The surface of the extended gate was subsequently rinsed with methanol and then dried with N<sub>2</sub> gas, resulting in self-assembled monolayers on the Au electrode.

### **Fabrication of the microfluidic chamber**

The microfluidic chamber was fabricated by casting PDMS on a silicon wafer that was treated by the dry etching process. The silicon wafer was fully covered with a negative photoresist material (SU-8 3050) by a spin coating method for 30 s at 1000 rpm. After the spinning process for 30 s at 3000 rpm

at r.t., the treated silicon wafer was soft-baked for 1 min at 65 °C and for 9 min at 95 °C. Next, UV irradiation for 20 s and then post-baking for 1 min at 65 °C and for 7 min at 95 °C were applied to form mold. After this period, the obtained substrate was treated by utilizing a photoresist material (SU-8 developer) for 5 min and subsequently rinsed with 2-propanol, followed by hard-baking for 10 min at 150 °C. The passivation layer of the silicon mold was formed by polytetrafluoroethylene, which was treated by RIE with  $\text{CHF}_3$  at 200 W and 50 sccm for 12 min.

Next, a crosslinking agent (Silpot 184 W/C) and PDMS were mixed at 1:9 (w/w) and centrifuged using planetary mixer equipment (THINKY, ARE 310 planetary centrifugal mixer) for 30 s at 2000 rpm. Bubbles generated from the mixture were removed by degassed treatment *in vacuo* for 15 min, and the mixture was subsequently cast on the silicon mold. After the baking process *in vacuo* for 1.5 h at 80 °C, the PDMS layer was disassembled from the silicon mold. The obtained microfluidic chamber made of PDMS was attached to the extended-gate electrode by the RIE treatment with  $\text{O}_2$  at 75 W and 50 sccm for 13 s and finally baked in an oven (AS ONE ETTAS AVO-200NB) for 1 h at 60 °C.

### 3. Characterization of the extended-gate electrode

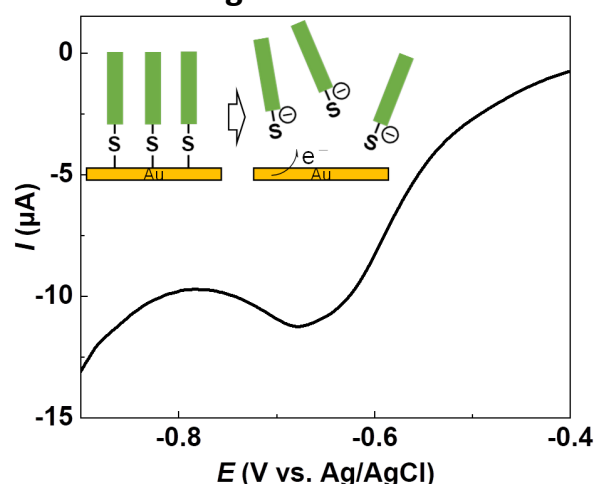


**Fig. S2** Result of the molecular density test by linear sweep voltammetry. The extended-gate electrode functionalized with 4-MPBA was evaluated in a KOH solution (0.1 M). The potential was applied from 0 V to -1.6 V, and the scan rate was set to be 20 mV/s. The molecular density of 4-MPBA-based SAM on the extended-gate electrode was determined based on Faraday's law with the integration of the peak area.

### 4. Electrical detection of $\text{H}_2\text{O}_2$

The gate electrode of the OFET was connected to the extended-gate electrode through a copper cable, which was evaluated under ambient conditions utilizing the semiconductor parameter analyzer. The gate voltage was applied through the Ag/AgCl reference electrode. In addition, almost no changes in transfer profiles in several repetitive measurements suggested its potential as a chemical sensor for stable detection of the analyte in aqueous media. The length, width, and height of the microfluidic chamber attached to the extended gate were 7 mm, 6 mm, and 50  $\mu\text{m}$ , respectively. The design and size of the fabricated microfluidic system were optimized for uniform diffusion of the aqueous solution<sup>2</sup> by utilizing a flow rate simulation of COMSOL Multiphysics software. The chamber was

connected to three inlets and one outlet, which could inject the solution and rinse the chamber easily. For the achievement of a highly uniform flow, the symmetrical hexagonal design was applied and corners of the chamber were removed.<sup>3</sup> A continuous measurement was carried out at a flow rate 46  $\mu\text{L}/\text{min}$ , which was regulated by the microfluidic pump equipped with the flow meter. The OFET device was operated at a constant voltage of gate ( $V_{\text{GS}} = -3 \text{ V}$ ) and drain ( $V_{\text{DS}} = -1 \text{ V}$ ).

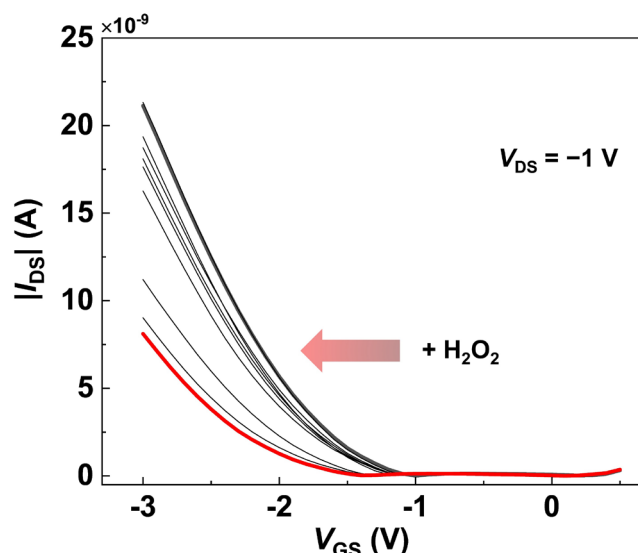


**Fig. S3** Changes of transfer characteristics the OFET-based sensor functionalized with 4-MPBA by adding  $\text{H}_2\text{O}_2$  (0–100  $\text{pg}/\text{mL}$ ) in ultrapure water.

**Table S1.** Comparison table for the limit of detection (LoD) values for  $\text{H}_2\text{O}_2$  detection.

Methods for $\text{H}_2\text{O}_2$ detection	LoD ( $\text{pg}/\text{mL}$ )	References
OFET-based sensor	0.71	This study
Electrochemical (polyaniline)	24	<i>Biosens. Bioelectron.</i> , 2014, <b>55</b> , 294.
Electrochemical (nanozyme)	$2.9 \times 10^3$	<i>J. Electroanal. Chem.</i> , 2021, <b>897</b> , 115603.
Electrochemical (gold nanoparticle)	$4.8 \times 10^4$	<i>J. Electroanal. Chem.</i> , 2019, <b>848</b> , 113359.
Electrochemical (gold nanoparticle)	1.1	<i>Anal. Chim. Acta.</i> , 2011, <b>701</b> , 75.
Electrochemical (silver nanoparticle)	$3.4 \times 10^4$	<i>ChemBioChem</i> , 2004, <b>5</b> , 1686.
Electrochemical (graphene oxide)	$3.0 \times 10^2$	<i>Nanoscale</i> , 2020, <b>12</b> , 5961.
Colorimetric (nanohybrid material by graphene oxide nanosheet, gold nanoparticles, and hyperbranched polyethylenimine)	72	<i>Anal. Chem.</i> , 2020, <b>92</b> , 3426
Colorimetric (nanoporphyrin combined with bromine)	$1.7 \times 10^4$	<i>Sens. Actuators, B</i> , 2021, <b>343</b> , 130104.
Fluorescent (nanoporous silicon-quinoline)	$1.5 \times 10^2$	<i>Sens. Actuators, B</i> , 2018, <b>276</b> , 466.
Fluorescent (MOF-based nanozyme)	$2.9 \times 10^2$	<i>Chem. Commun.</i> , 2018, <b>54</b> , 1762.

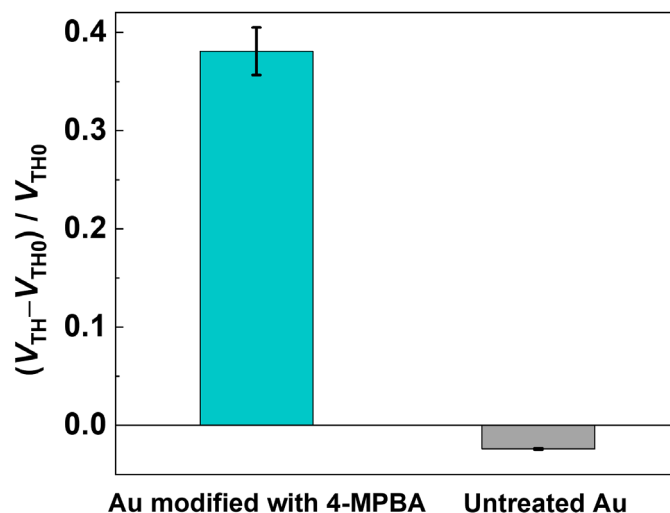


**Fig. S4** Difference in  $V_{TH}$  of the OFET with untreated electrode or the 4-MPBA modified extended-gate-electrode upon the addition of  $H_2O_2$  (100  $\mu g/mL$ ).

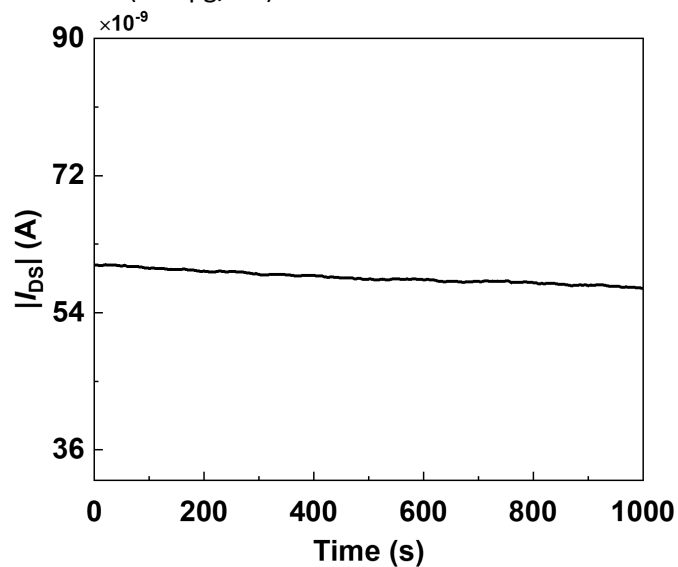


**Fig. S5** The stability test of the integrated OFET with the microfluidic chamber at a flow rate 46  $\mu L/min$ .

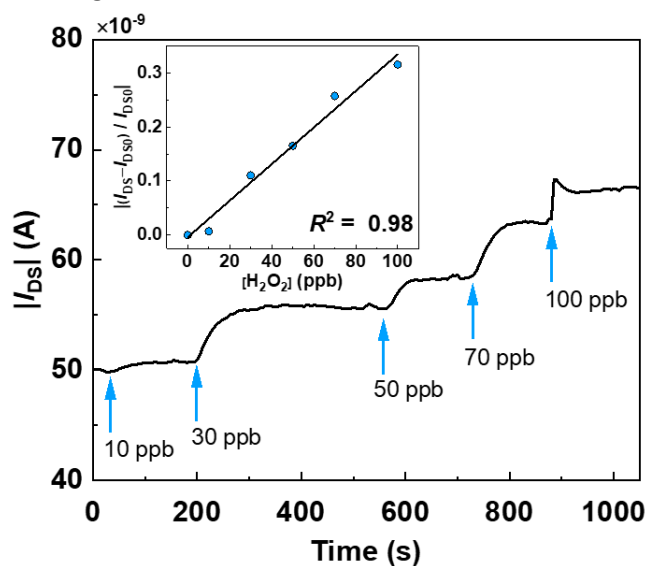


**Fig. S6** Real-time monitoring of the  $I_{DS}$  change by adding the different concentration of  $H_2O_2$ .

## 5. DFT Calculation of dipole moment

The DFT calculation was operated by Gaussian 16 Revision C.01.<sup>4</sup> Each structure of 4-MPBA and 4-HBT was optimized and calculated at the B3LYP(D3BJ)/def2SVP<sup>5-9</sup> level for generating the wave function files, which was analyzed with Multiwfn 3.8.<sup>10</sup> After this process, the dipole moment with Visual Molecular Dynamics (VMD) 1.9.4.<sup>11</sup> was finally visualized.

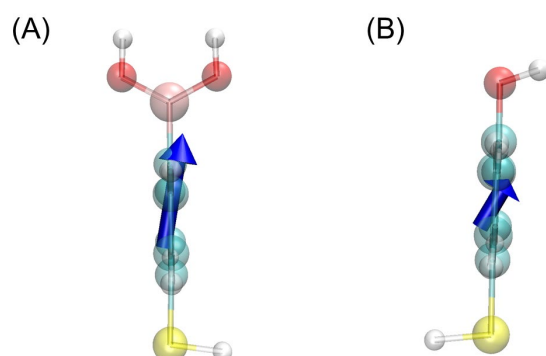


Fig. S7 DFT calculation result of the dipole moment of (A) 4-MPBA and (B) 4-HBT.

## 6. Investigation of the functionalized extended gate after the oxidation

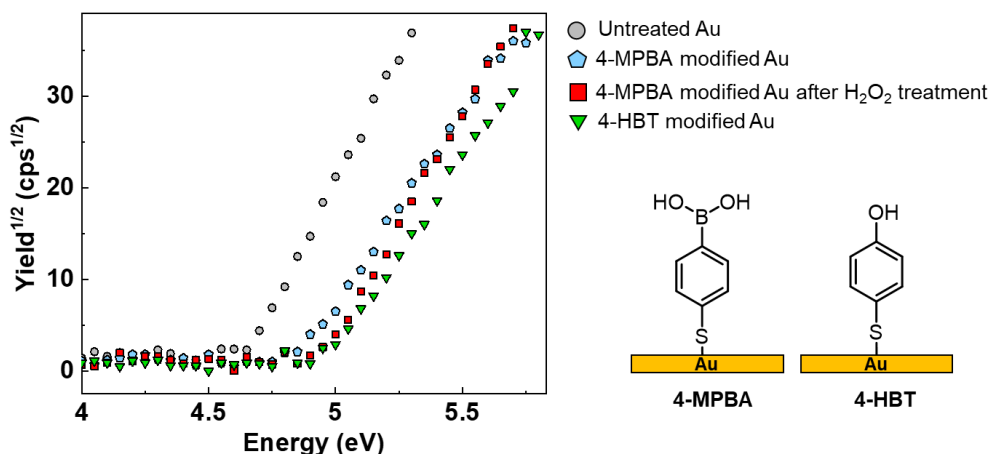


Fig. S8 Results of photoelectron yield spectroscopy measurements in air. Each plot represents the untreated Au electrode (black circle) and the treated Au electrodes by 4-MPBA (blue pentagon) or 4-HBT (green lower triangle). The 4-MPBA modified Au electrode was treated with  $\text{H}_2\text{O}_2$  (red square).

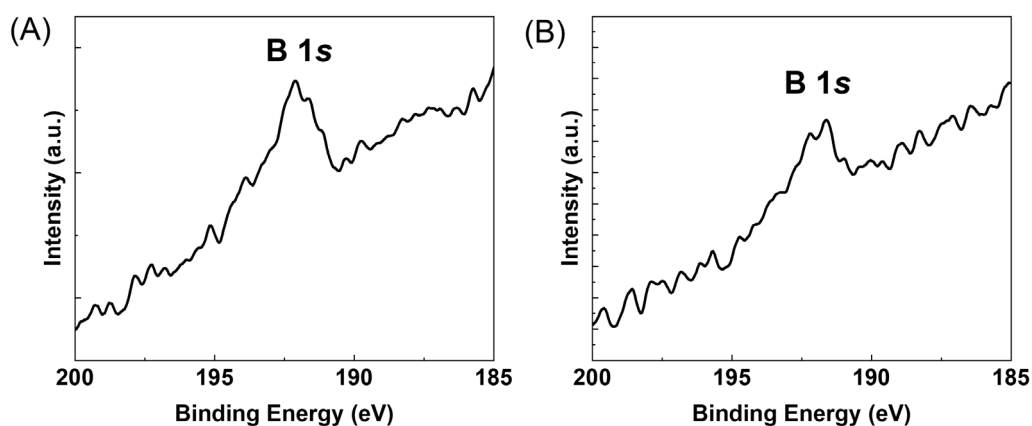
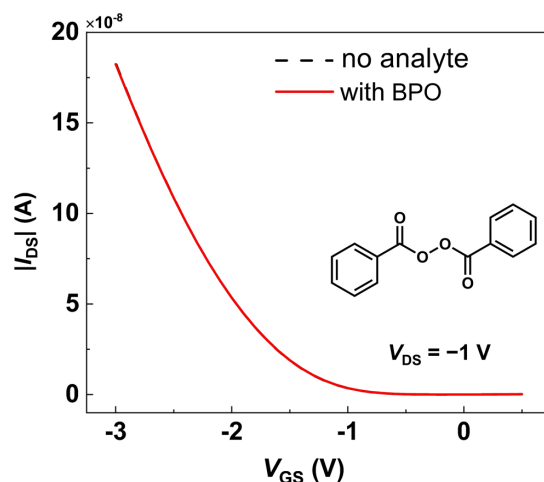
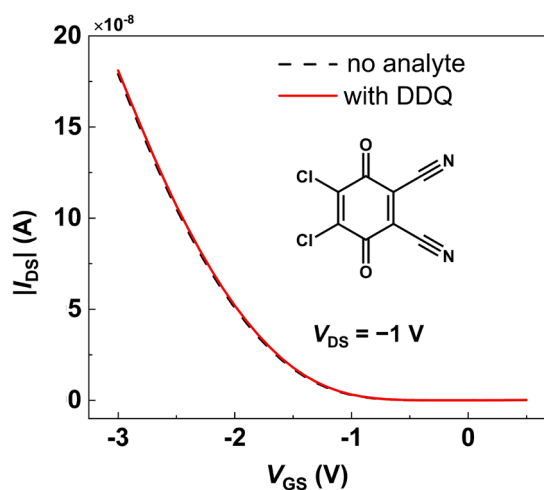


Fig. S9 XPS measurement of the Au electrode modified with 4-MPBA (A) before and (B) after the  $\text{H}_2\text{O}_2$  treatment. The decrease of the relative atomic concentration ratio (*ca.* 10 %) at B 1s was observed by comparing the area ratio of B 1s and S 2p.

## 7. Selectivity



**Fig. S10** Transfer characteristics of the OFET functionalized with 4-MPBA by adding benzoyl peroxide (BPO) (100 pg/mL) in ultrapure water.



**Fig. S11** Transfer characteristics of the OFET functionalized with 4-MPBA by adding 2,3-dichloro-5,6-dicyano-1,4-benzoquinone (DDQ) (100 pg/mL) in ultrapure water.

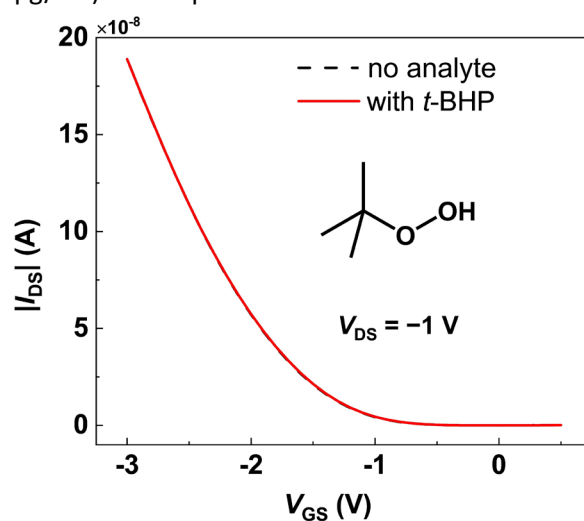


**Fig. S12** Transfer characteristics of the OFET functionalized with 4-MPBA by adding *tert*-butyl hydroperoxide (DDQ) (100 pg/mL) in ultrapure water.

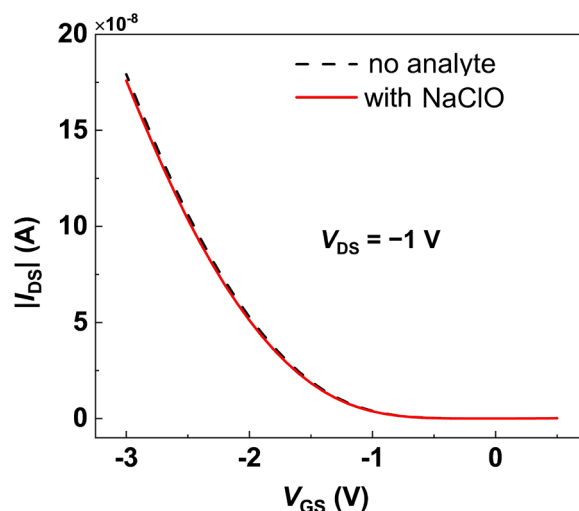


**Fig. S13** Transfer characteristics of the OFET functionalized with 4-MPBA by adding sodium hypochlorite (100 pg/mL) in ultrapure water.

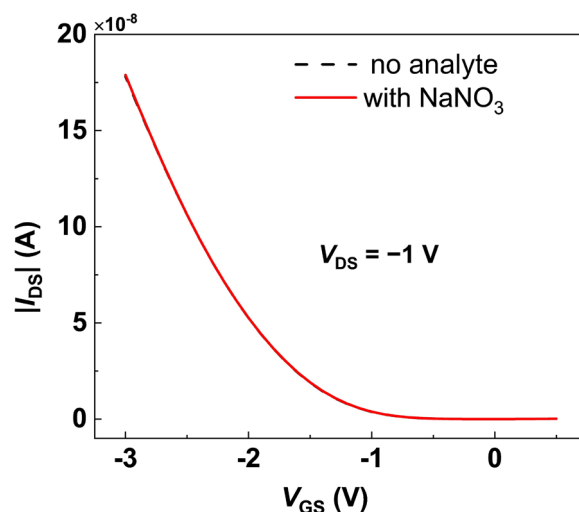


**Fig. S14** Transfer characteristics of the OFET functionalized with 4-MPBA by adding sodium nitrate (100 pg/mL) in ultrapure water.

## References

1. H. J. Queisser and D. E. Theodorou, *Phys. Rev. B*, 1986, **33**, 4027-4033.
2. J. Zhang, S. Yan, D. Yuan, G. Alici, N.-T. Nguyen, M. E. Warkiani and W. Li, *Lab Chip*, 2016, **16**, 10-34.
3. P. Didier, N. Lobato-Dauzier, N. Clément, A. J. Genot, Y. Sasaki, É. Leclerc, T. Minamiki, Y. Sakai, T. Fujii and T. Minami, *ChemElectroChem*, 2020, **7**, 1332-1336.
4. M. J. Frisch, G. W. Trucks, H. B. Schlegel, G. E. Scuseria, M. A. Robb, J. R. Cheeseman, G. Scalmani, V. Barone, G. A. Petersson, H. Nakatsuji, X. Li, M. Caricato, A. V. Marenich, J. Bloino, B. G. Janesko, R. Gomperts, B. Mennucci, H. P. Hratchian, J. V. Ortiz, A. F. Izmaylov, J. L. Sonnenberg, D. Williams-Young; ; F. Ding, F. Lipparini, F. Egidi, J. Goings, B. Peng, A. Petrone, T. Henderson, D. Ranasinghe, V. G. Zakrzewski, J. Gao, N. Rega, G. Zheng, W. Liang, M. Hada, M. Ehara, K. Toyota, R. Fukuda, J. Hasegawa, M. Ishida, T. Nakajima, Y. Honda, O. Kitao, H. Nakai, T. Vreven, K. Throssell, J. A. Jr. Montgomery, J. E. Peralta, F. Ogliaro, M. J. Bearpark, J. J. Heyd, E. N. Brothers, K. N. Kudin, V. N. Staroverov, T. A. Keith, R. Kobayashi, J. Normand, K.

Raghavachari, A. P. Rendell, J. C. Burant, S. S. Iyengar, J. Tomasi, M. Cossi, J. M. Millam, M. Klene, C. Adamo, R. Cammi, J. W. Ochterski, R. L. Martin, K. Morokuma, O. Farkas, J. B. Foresman and D. J. Fox, Gaussian 16 (Revision. C.01), Gaussian Inc., Wallingford, CT, 2016 (accessed February 28, 2022).

5. A. D. Becke, *Phys. Rev. A*, 1988, **38**, 3098-3100.
6. A. D. Becke, *J. Chem. Phys.*, 1993, **98**, 5648-5652.
7. C. Lee, W. Yang and R. G. Parr, *Phys. Rev. B*, 1988, **37**, 785-789.
8. S. Grimme, J. Antony, S. Ehrlich and H. Krieg, *J. Chem. Phys.*, 2010, **132**, 154104.
9. B. P. Pritchard, D. Altarawy, B. Didier, T. D. Gibson and T. L. Windus, *J. Chem. Inf. Model.*, 2019, **59**, 4814-4820.
10. T. Lu and F. Chen, *Comput. Chem.*, 2012, **33**, 580-592.
11. W. Humphrey, A. Dalke and K. Schulten, *J. Mol. Graphics*, 1996, **14**, 33-38.